Journal of Power Sources 206 (2012) 429–435

Contents lists available at SciVerse ScienceDirect

Journal of Power Sources

journal homepage: www.elsevier.com/locate/jpowsour

Analysis of pressure variations in a low-pressure nickel–hydrogen battery: Part 1

B.K. Purushothaman*, J.S. Wainright

Department of Chemical Engineering, Case Western Reserve University, 10900 Euclid Avenue, Cleveland, OH 44106, USA

ARTICLE INFO

Article history:
Received 16 January 2012
Received in revised form 27 January 2012
Accepted 27 January 2012
Available online 7 February 2012

Keywords:
Nickel hydrogen battery
State of charge
Fuel gauging
Metal hydride
Pressure analysis

ABSTRACT

A low pressure nickel–hydrogen battery using either a metal hydride or gaseous hydrogen for H_2 storage has been developed for use in implantable neuroprosthetic devices. In this paper, pressure variations inside the cell for the gaseous hydrogen version are analyzed and correlated with oxygen evolution side reaction at the end of charging, the recombination of oxygen with hydrogen during charging and a subsequent rest period, and the self-discharge of the nickel electrode. About 70% of the recombination occurred simultaneously with oxygen evolution during charging and the remaining oxygen recombined with hydrogen during the 1st hour after charging. Self-discharge of the cell varies linearly with hydrogen pressure at a given state of charge and increased with increasing battery charge levels. The coulometric efficiency calculated based on analysis of the pressure–time data agreed well with the efficiency calculated based on the current–time data. Pressure variations in the battery are simulated accurately to predict coulometric efficiency and the state of charge of the cell, factors of extreme importance for a battery intended for implantation within the human body.

1. Introduction

Currently, there is a large array of neuroprosthetic devices being developed by researchers around the world to provide electric stimulation to paralyzed muscles. These devices supply electrical currents to intact motor nerves thereby restoring function and enhancing the lives of patients with spinal cord injuries such as paraplegics and quadriplegics. These devices assist the users with daily activities like breathing (diaphragm stimulators) standing, stepping, reaching and grasping. Neural stimulation has also been applied to control appetite, restore vision with retinal implants and to aid hearing with cochlear implants [1]. Two common methods of stimulation are surface stimulation (stimulation outside the body) and percutaneous stimulation (stimulation inside the body). Typical percutaneous stimulators employ electrodes implanted within the muscles that are energized via radio-frequency energy transfer. An external battery pack and RF generator are worn by the user, and careful placement of the external FR coil is required in order to transfer sufficient electrical energy for stimulation to occur. A next generation neuroprosthetic system currently being developed at Case Western Reserve University will be completely implantable and can be employed for different clinical applications due to its open architecture. The advantages of an implantable system are repeatability (no RF link to maintain in operation), cosmetics (no external devices to be worn) and flexibility [2]. Unlike implantable pacemakers, whose power requirements can be met with low power (μW) primary batteries, the power requirements for these neuroprosthetic devices are substantial (100s of mW). This requires a rechargeable power source, given the limited volume available within the body for the battery. In addition, an exceptionally long life, both in terms of calendar life and cycle life is required, as most spinal cord injury patients are relatively young, and have a life expectancy of over 40 years after their injury.

Nickel hydrogen batteries are currently used in many aerospace and satellite applications, as their cycle life greatly exceeds that of any other secondary battery technology (20,000–60,000 cycles as opposed to 500–2000 for most other technologies) [3–6]. In addition, they are uniquely tolerant to fault conditions (overcharge, overdischarge, shorting) leading to inherent safety, and the hydrogen pressure provides a direct measure of the battery state of charge (SOC) [3]. To a great extent, these factors minimize the 'watch-dog' circuitry typically required for rechargeable batteries, simplifying the overall system and greatly increasing reliability and safety.

The low pressure nickel hydrogen battery developed in this work uses either gas phase hydrogen storage or a metal hydride to store the hydrogen gas. The metal hydride version is described in detail in part II of this paper. Nickel hydrogen batteries developed for aerospace applications typically employ gas phase hydrogen storage at pressures of 40–65 × 10^5 Pa (600–1000 psia). For the implantable application considered here, operation at similar

* Corresponding author. Present address: Medtronic, Mounds View North Facility, 8200 Coral Sea Street NE, MVN51, Mounds View, MN 55112, USA.
Tel.: +1 763 526 0193; fax: +1 763 526 5737.
E-mail addresses: bushan.k.purushothaman@medtronic.com, bushan@gmail.com (B.K. Purushothaman).

0378-7753/$ – see front matter © 2012 Elsevier B.V. All rights reserved.
doi:10.1016/j.jpowsour.2012.01.150

Nomenclature

F	Faraday constant, 96,485 C/equiv.
k	recombination rate constant, s^{-1}
Δn	change in number of moles
η_c	coulometric efficiency
P	pressure, psi
ΔP	change in pressure, psi
Q	capacity, Ah
R	gas constant, J $(mol\,K)^{-1}$
t	time, s
T	temperature, K
V	volume, cm^3
Z	number of electrons transferred in a faradic reaction, equiv./mole

Subscripts

charge	charge phase
discharge	discharge phase
H_2	hydrogen gas
o	initial
O_2	oxygen gas
Recom	recombination
SD	self discharge

pressures represented a significant safety hazard in the event of a pressure shell failure, and an unwelcome constraint on the geometry of the battery. Spacecraft cells are typically spherical or cylindrical with hemispherical ends in order to minimize the weight of the pressure shell, whereas for implant applications, a prismatic shape is generally preferred.

The major difference between the low pressure nickel hydrogen battery and a conventional Ni–MH battery is that cycle and calendar life of the former can be much greater, since the negative electrode is purely catalytic in nature. Side reactions associated with corrosion of the metal hydride are eliminated, as are changes in the shape and volume of the negative electrode.

The low pressure nickel–hydrogen battery has one other significant advantage with respect to a conventional Ni–MH cell. This advantage is derived from to the ability to monitor the hydrogen pressure within the cell. From the hydrogen pressure, it is possible to directly monitor the battery capacity remaining (i.e., fuel gauging) including accounting for the effects of self-discharge and overcharging.

In this work, several factors that affect the cell performance including (a) self-discharge, (b) oxygen evolution, and (c) oxygen–hydrogen recombination, and how these can be evaluated from the pressure–time behavior of the low pressure Ni–H_2 cell will be discussed. In this paper results are presented for a battery without a metal hydride component, while in part II, the behavior of a battery with metal hydride storage will be presented.

2. Experimental

A schematic picture of the nickel hydrogen battery is shown in Fig. 1. The pre-formed nickel hydroxide positive electrode and the platinum catalyzed negative electrode were separated by a polypropylene membrane (Celgard 3400 from Celgard, Charlotte, NC, USA) soaked in 26 wt% KOH were assembled using a single nylon bolt down the middle of the electrode discs. Nickel mesh served as both current collector (for the positive electrode) and as a gas diffusion layer for the negative electrode. The negative electrode (E-tek, A2, 10% Pt/C on a Ag plated Ni screen, 0.6 mg Pt cm^{-2} from E-tek Corporation, Somerset, NJ, USA) was soaked for 24 h

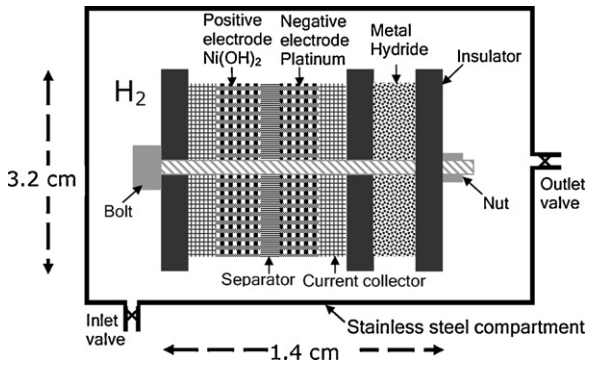

Fig. 1. Schematic picture of the Ni–H_2 cell with metal hydride.

in 26 wt% KOH prior to assembly. The electrode discs were 2.5 cm in diameter, the central hole for the bolt was 0.4 cm in diameter. Two chlorinated polyvinyl chloride (CPVC) discs, 3.2 cm in diameter, at the ends of the cell provide electrical insulation from the pressure vessel. The cell was housed in a stainless steel cylinder filled with hydrogen gas to the desired pressure. The inlet and outlet valves shown are used for purging and filling the cell to the desired hydrogen pressure.

The pressure inside the cell, typically in the range 1–3 atmospheres, was monitored using a pressure gauge (Omega Inc., PX 300 series, Stamford, CT, USA). The accuracy of the pressure gauge according to manufacturer's specifications is ±0.025 psi. A National Instruments data acquisition card was used to data-log the pressure signal. As the cell is charged or discharged the pressure is recorded simultaneously along with the voltage and current.

The nickel hydroxide positive electrode was fabricated in-house. Uniform, high purity nickel foam from INCO was used as a substrate. The thickness of the nickel foam was 1.6 mm and the density is about 420 g m^{-2}. The number of pores per inch is 110. Nickel hydroxide powder from Kansai Catalyst Corporation LTD was used as the active material. The composition of this nickel hydroxide formulation as obtained is 54% Ni, 3.2% Co and 4.5% Zn. According to the product information, 4.5% Zn and 0.7% Co were mixed as a solid solution with nickel hydroxide. These particles were then coated with 2.5% Co. The cobalt coating is a mixture of cobalt hydroxide and cobalt oxyhydroxide. The average size of the nickel hydroxide particles was about 12 μm. The active material was blended with a binder and a solvent using a homogenizer. The binder was polyvinylidene fluoride (PVDF, Kynar 2800 from ARKEMA Inc., PA, USA) and the solvent was N-methyl pyrrolidone. The binder provides adhesion of particles to one another and to the substrate. Filamentary nickel powder (INCO type 210, 0.5–1 μm from Novamet, Wyckoff, NJ, USA) was used as a filler to enhance the conductivity of the paste. A screen printer was used to mechanically press the active paste into the nickel foam substrate. The nickel foam with paste was then dried in vacuum at 100 °C overnight to remove the solvent.

To form the positive electrode, the Ni foam containing the nickel hydroxide paste was soaked in 26 wt% KOH overnight and then cycled at a C/20 rate (based on the theoretical capacity of the electrode) for 5 cycles, after which a reproducible charge/discharge voltage profile was obtained. The electrode contained 8.7% PVDF, 8.8% nickel and the rest $Ni(OH)_2$ on a dry weight basis and had a theoretical capacity of 17.7 mAh cm^{-2}. The coulometric efficiency of this electrode when charged completely at a C/5 rate was 89.3%. Coulometric efficiency was calculated as the ratio of the capacity obtained during discharge to the capacity passed during charge. When charged to a capacity of 14.3 mAh cm^{-2}, the coulometric efficiency of the electrodes increased to 93–96% due to the decrease in the oxygen evolution at the end of charging. The experimental

capacity of the electrode was therefore taken as 14.3 mAh cm^{-2}. All 'C'-rates in this paper are referred to this value.

3. Reactions involved

During charge, nickel hydroxide is oxidized to nickel oxyhydroxide at the positive electrode according to Eq. (1). The reverse of the reaction occurs during discharge.

$$Ni(OH)_2 + OH^- \underset{\text{discharge}}{\overset{\text{charge}}{\rightleftarrows}} NiOOH + H_2O + e^- \quad (1)$$

At the platinum negative electrode, hydrogen is formed by electrolysis of water during charge and the hydrogen gas is oxidized during discharge according to Eq. (2).

$$H_2O + e^- \underset{\text{discharge}}{\overset{\text{charge}}{\rightleftarrows}} \frac{1}{2}H_2 + OH^- \quad (2)$$

The net reaction in the cell during charge and discharge is:

$$Ni(OH)_2 \underset{\text{discharge}}{\overset{\text{charge}}{\rightleftarrows}} NiOOH + \frac{1}{2}H_2 \quad (3)$$

The concentrations of hydroxyl ion and water remain constant in the cell at all states of charge.

3.1. Overcharge

When the cell is overcharged, oxygen is evolved at the nickel hydroxide positive electrode (Eq. (4)) and there is no change in reaction at the platinum negative electrode (Eq. (2)). The evolved oxygen recombines with hydrogen at the platinum electrode according to Eq. (5). Because of this recombination, there is no change in the hydroxyl ion and water concentrations in the cell thereby making these cells very tolerant to abuse conditions.

$$2OH^- \overset{\text{+ve electrode}}{\longrightarrow} \frac{1}{2}O_2 + H_2O + 2e^- \quad (4)$$

$$H_2 + \frac{1}{2}O_2 \Rightarrow H_2O + \text{heat} \quad (5)$$

3.2. Over-discharge

When the cell is over-discharged, hydrogen is generated at the positive electrode and is consumed at the negative platinum electrode, without any change in pressure in the nickel–hydrogen cell. Again, the net amount of KOH and water in the cell does not change on over-discharge.

4. Results and discussion

4.1. Coulometric efficiency analysis

The coulometric efficiency is one of the important parameters used to gauge the performance of the nickel–hydrogen cells and to understand the efficiency loss due to oxygen evolution as a side reaction (Eq. (4)) during charging. The coulometric efficiency was investigated for the low pressure nickel hydrogen cell cycled at a C/5 rate to different states of charge, which is defined here as the "amount of charge applied to the cell from a state of complete discharge". The end of discharge is based on a cut-off voltage of 1.15 V, which was determined by the knee at the end of the discharge profile (Fig. 2). The coulometric efficiency decreases with an increase in the SOC as expected (Table 1) due to the increase in oxygen evolution at higher charging potentials.

It is also well known that the nickel–hydrogen cells suffer from self discharge due to reduction of nickel oxyhydroxide to nickel hydroxide in the presence of hydrogen gas and KOH electrolyte [3]. The self discharge rate is directly proportional to the hydrogen gas pressure inside the cell. Monitoring and understanding the self discharge is therefore critical to the development of a practical battery.

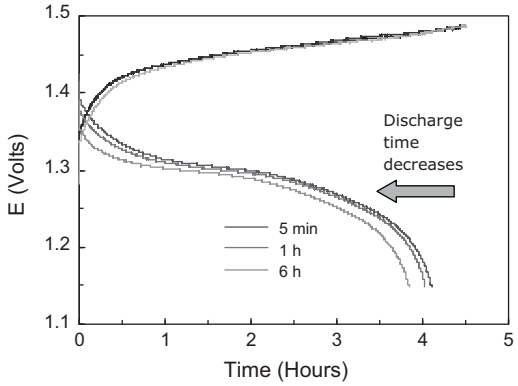

Fig. 2. Charge–discharge voltage profiles of the nickel–hydrogen cell cycled at C/5 rate to 90% SOC with different rest periods, 5 min, 1 h and 6 h.

In comparison to that observed in high pressure nickel hydrogen batteries used in space applications the self-discharge in our low pressure nickel hydrogen battery should be lower, because of the lower operating pressure (≈30 psia). The self discharge phenomenon was studied by introducing a rest period between charge and discharge. The rest period was varied and the coulometric efficiency was calculated. The voltage profiles during charge and discharge of the nickel–hydrogen cell with different rest periods, (5 min, 1 h and 6 h), are shown in Fig. 2. It is evident that the discharge time decreases with an increase in the rest period, indicating that the low pressure nickel–hydrogen cell does undergo self-discharge. This results in decreased coulometric efficiency with an increase in the rest period as detailed in Table 1.

4.2. Pressure variations analysis

The voltage variations during the charge, rest, and the discharge periods of the cell cycled at C/5 rate to 90% SOC are shown in Fig. 3A. The rest period in this case is about 6 h. It is evident from the figure that the voltage increases during charge, followed by relaxation of the voltage during the rest period. Subsequently, during discharge the voltage drops until the cut-off voltage of 1.15 V is reached followed by relaxation of the voltage during the rest period for 6 h. The change in slope of the voltage vs time plot near the end of charge corresponds to the onset of oxygen evolution in addition to charging, and is clearly evident in Fig. 3A.

The cell pressure was measured simultaneously during the charge–discharge cycle and is shown in Fig. 3B. The pressure inside the cell increases during charge due to the formation of hydrogen at the platinum electrode (Eq. (2)). The rate of pressure increase is linear and corresponds to the current applied to the cell. Based on the pressure change and charge passed, the gas volume inside the cell was estimated at 42 cm^3. During the rest period, the pressure is not constant as one might expect; instead a decrease in the

Table 1
Coulometric efficiency of the Ni–H_2 cell as a function of SOC cycled at C/5 rate.

SOC (%)	Efficiency for different rest periods (%)		
	5 min	1 h	6 h
50	95.5	93.9	89.2
70	94.2	93.1	87.5
90	91.2	89.7	85.4

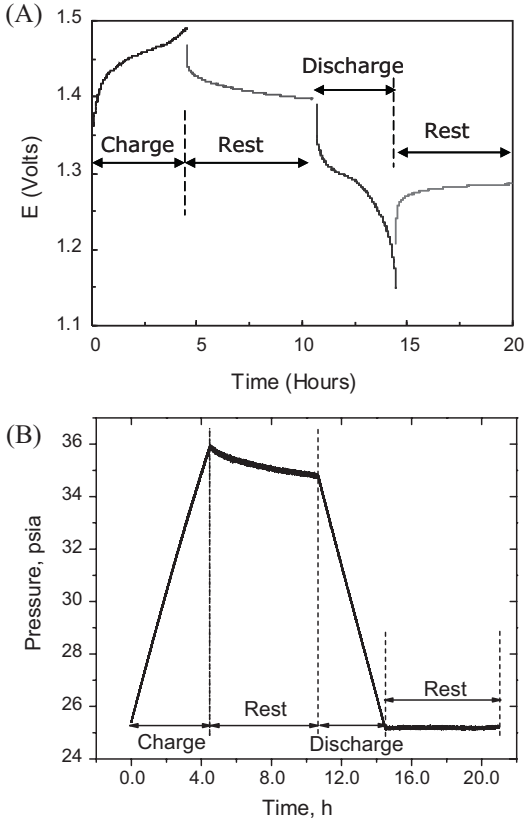

Fig. 3. Voltage (A) and pressure (B) variations during charge, rest and discharge periods of a cycle. The cell was cycled at C/5 rate to 90% SOC. The rest period is 6 h.

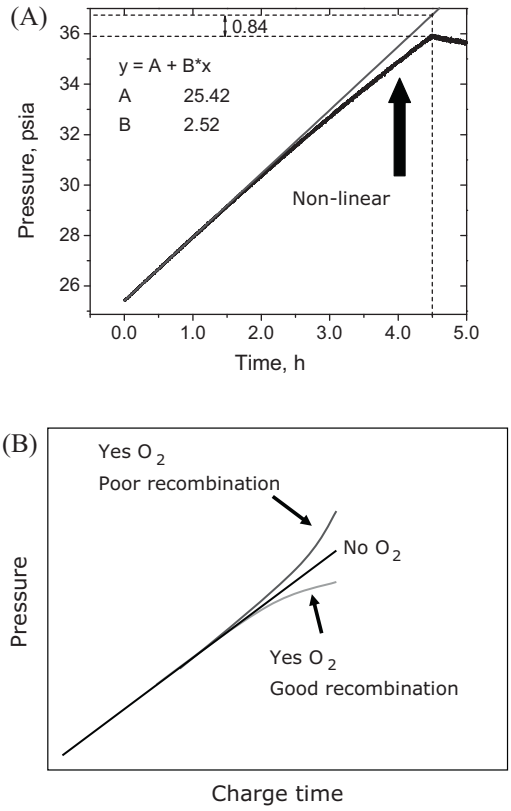

Fig. 4. (A) Changes in pressure during the charge. The cell was cycled at C/5 rate to 90% SOC. (B) Schematic representation of different pressure variations due to different possible mechanisms during charging.

hydrogen pressure is seen. This decrease in pressure can be accounted for by two mechanisms: (a) recombination of evolved oxygen with hydrogen at the platinum electrode and (b) self discharge of the nickel electrode with consumption of hydrogen. In reality, the pressure decrease is a combination of both mechanisms and will be discussed in detail below. The pressure decreases linearly during discharge because of the hydrogen oxidation at the platinum electrode (Eq. (2)). During the rest period after discharge, no significant change in pressure is observed as shown in Fig. 3B.

4.2.1. Pressure variations during charge

The pressure inside the cell as a function of the charge time is shown in Fig. 4A. The pressure variation during the first hour of charging was fit to a straight line, $y = A + B \times x$. The slope of the linear fit (parameter B), 2.52 psi h^{-1}, in Fig. 4A corresponds to the rate of formation of hydrogen and is consistent with the charging current (15.6 mA), the volume of the cell (42 cm^3) and room temperature (25 °C). The effect of temperature variation on the pressure rate is considered negligible in comparison to pressure changes due to hydrogen evolution. It is evident that the pressure variation towards the end of the charging phase is non-linear when compared to the straight line fit.

A schematic representation of possible variations in pressure during charge is shown in Fig. 4B. At short charge times, it is assumed there is no significant oxygen evolution and that all current goes to the main reaction which is oxidation of nickel hydroxide to nickel oxyhydroxide (Eq. (1)). Therefore the pressure increases linearly corresponding to the rate of hydrogen formation as shown by a straight line marked as 'No O_2' in Fig. 4B, which assumes that there is no oxygen evolution.

In reality, as evident in the voltage profile change at the end of charging (Fig. 3A) part of the current to the nickel hydroxide electrode goes to oxygen evolution, the side reaction. Therefore in addition to hydrogen evolution in the platinum electrode, there is also oxygen evolution in the nickel hydroxide electrode causing a steep rise in pressure as shown by the curve marked as 'Yes O_2 Poor recombination' in Fig. 4B. It is assumed here that the recombination of oxygen with hydrogen is slow and oxygen builds up in the gas phase.

However, if the oxygen evolved at the nickel hydroxide electrode recombines rapidly with the hydrogen evolved at the platinum electrode, a decrease in the rate of pressure rise will be evident as shown by the curve marked as 'Yes O_2 Good recombination' in Fig. 4B. It is evident by comparing Fig. 4A and B that the evolved oxygen does recombine with hydrogen during charging. This is evident from the difference in the predicted pressure based on the linear fit and the measured pressure at the end of 4.5 h, which is about −0.84 psi. This indicates that the measured pressure at the end of the charge period (4.5 h) is mostly hydrogen plus a small amount of the oxygen that has not yet recombined.

4.2.2. Pressure variations during the rest period

The pressure in the cell decreases monotonously during the rest period as shown in Fig. 5A. This pressure drop when no charge or discharge current is applied to the cell is due to (a) the recombination of oxygen with hydrogen gas and (b) the self discharge of the cell. The leftover oxygen gas that was not recombined during the charge period recombines at the Pt electrode. The self discharge occurs due to the oxidation of the hydrogen gas at the nickel electrode and reduction of nickel oxyhydroxide to nickel hydroxide. Both these processes result in the decrease of hydrogen pressure in the cell. It is noted that the noise in the pressure data is due to 60 Hz electrical noise introduced during the analog to digital conversion by the data acquisition card.

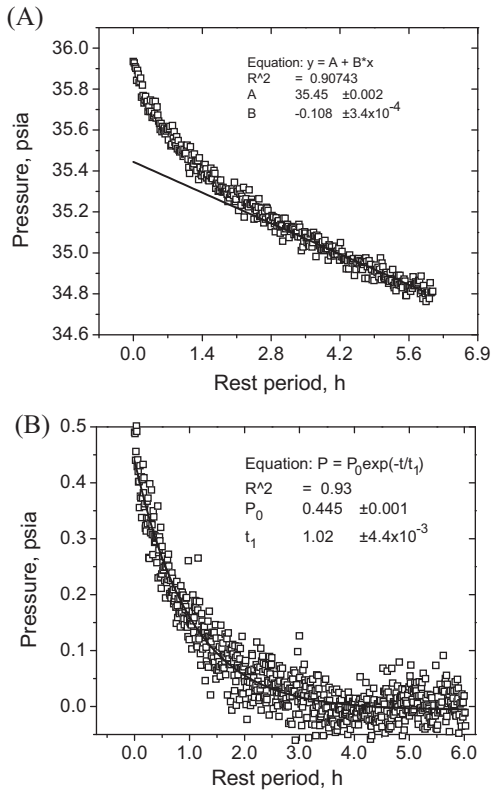

Fig. 5. Pressure changes during the rest period. The cell was cycled at C/5 rate to 90% SOC. (A) A straight line is fit to the pressure data from 3 to 6 h in the rest period and extrapolated back to time 0. (B) Pressure changes due to recombination reaction during the rest period. An exponential decay line is fit to the pressure data.

The self discharge rate can be assumed to be constant at a given SOC of the battery. Therefore the hydrogen pressure in the cell will decrease linearly with rest time as a result of self discharge. It is also evident from Fig. 5A that the pressure change is linear in the rest period from 3 to 6 h and therefore it is assumed that all oxygen recombination is complete in the first 3 h of the rest period. A linear fit to the pressure data in the time period, 3–6 h is shown in Fig. 5A. The error calculated for the linear fit is very small. The slope of the line, or the rate of the pressure change, is 0.108 psi h^{-1}. This self discharge rate is about 23 times slower than the charge rate (C/5). At this rate, the cell will discharge completely in about 117 h and the self discharge rate could be expressed as C/117. In principle, the self discharge rate is not constant and decreases with decreasing SOC, and therefore the cell will last significantly longer than 117 h. Based on the self discharge rate, the drop in pressure due to self discharge is about 0.648 psi during the time period shown in Fig. 5A.

The pressure contribution due to the self discharge of the cell during the rest period based on the linear fit was subtracted from the total pressure data and the difference, the pressure contribution due to the recombination reaction, is plotted in Fig. 5B. The pressure variation due to the recombination reaction follows an exponential decay and the pressure changes are nearly complete in 2 h. The recombination of oxygen with hydrogen gas is considered to be a first order reaction in oxygen and zero order in hydrogen due to hydrogen excess in the cell. The rate equation for the recombination reaction is then:

$$\frac{dp}{dt} = -kP \tag{6}$$

where P is the pressure of oxygen and k is the rate constant.

The solution to this rate equation is:

$$P = P_0 \exp(-kt) \tag{7}$$

Table 2
Pressure loss contributions of recombination during charge and subsequent 6 h rest period.

Recombination Pressure drop	50% SOC	70% SOC	90% SOC
Charge, psi	0.13	0.14	1.03
Rest period, psi	0.09	0.11	0.45
Charge, %	57.9	65.2	66.1
Rest period, %	42.1	34.8	33.9

where P_0 is the initial pressure of oxygen. The above solution is in the form of an exponential decay. Therefore the pressure drop due to the recombination reaction was fitted to an exponential decay equation as shown in Fig. 5B. An excellent fit with low error values is obtained. The parameter P_0 represents the total pressure drop due to the recombination reaction during the rest period and is 0.445 psi. The pressure drop due to the self discharge (0.648 psi) and that due to the recombination are of the same order of magnitude and therefore neither one can be neglected. The time constant t_1 (i.e. k^{-1} in Eq. (7)) is 1.02 h. In comparison, the time constant for the recombination reaction obtained with just the platinum electrode present in the pressure vessel in a separate experiment, is about 15 min. This difference in time indicates that the recombination process in the nickel hydrogen cell is limited by the diffusion of oxygen from the nickel hydroxide electrode to the platinum electrode.

4.2.3. Recombination amounts during charge and rest period

The difference in the predicted pressure based on the linear fit and the measured pressure at the end of the charge as described in Section 4.2.1 was calculated for different states of charge. This decrease in pressure is due to the recombination of hydrogen gas with oxygen gas and will be referred to as the pressure drop due to recombination [$\Delta P(H_2/O_2)$] during the charge period. It is noted here that only a fraction of oxygen formed is recombined during the charging period and the remaining fraction recombines during the rest period. The pressure drop due to the recombination reaction in the rest period was calculated by fitting an exponential decay equation as described in Section 4.2.2.

The pressure drop due to recombination as a function of SOC during charging and the rest period is listed in Table 2. The pressure drop due to the recombination during the charge and rest periods increases with increase in the SOC. Assuming that the recombination rate is the same at all states of charges, the pressure drop contributions indicate that the oxygen evolution increases and therefore the recombination increases with the SOC. This increase in oxygen evolution agrees well with the coulometric efficiency results, which show a decrease in efficiency with increase in SOC.

Comparing the pressure drops in the charge and the rest periods, it is evident that about 58–66% of the recombination is complete during the charge period for different SOCs (Table 2) and this clearly shows good recombination on the platinum electrode. The rate constant obtained for the recombination reaction is about the same, 0.94 h^{-1}, for all states of charge. This indicates that all the recombination is complete during the first 1 h of the rest period and suggests the importance of providing rest periods after charge in order to keep water balanced in this nickel hydrogen cell.

4.2.4. Self discharge at different states of charge

The self discharge rate was determined by the linear fit described in Section 4.2.2 and was found to increase with SOC. The self discharge rate at 50% SOC is 0.068 psi h^{-1} and corresponds to a rate of C/180. For the 70% and 90% SOC, the self discharge rate was about C/117 and C/90, respectively.

Table 3
Pressure loss contributions of recombination and self discharge for 6 h rest period between charge and discharge.

Pressure drop	50% SOC	70% SOC	90% SOC
Recombination, psi	0.22	0.62	1.48
Self discharge, psi	0.41	0.68	0.77
Recombination, %	34.6	47.9	65.7
Self discharge, %	65.4	52.1	34.3

4.2.5. Pressure contributions – self discharge and recombination

The net pressure loss due to self discharge and recombination at different states of charge for the nickel–hydrogen cell is listed in Table 3. The rest period between charge and discharge was 6 h. It is evident that the pressure loss due to the total recombination (including charge and rest) and self discharge increases with the SOC. In terms of percentage loss, the self discharge contribution decreases with SOC. This indicates that the oxygen evolution is the major mechanism for pressure loss at high states of charges and the self discharge is the major mechanism for pressure loss at shallow states of charges for the 6 h rest periods.

For the 5 min and 1 h rest periods, oxygen evolution is the predominant factor for all SOC as the time for self-discharge is small.

4.3. Simulation of pressure variations in charge discharge cycle

The pressure variation of the low pressure nickel hydrogen battery was simulated during charge, rest period and discharge from the initial pressure considering typical recombination and self discharge processes derived in the previous sections. The measured and simulated pressure of the battery cycled at C/5 rate to 90% SOC with 5 min rest period is shown in Fig. 6. The pressure increase during charging was simulated considering the hydrogen evolution based on Faraday's law and ideal gas law and the recombination of oxygen with hydrogen based on the pressure fit curve obtained from a different cycle at C/5 charging rate. The recombination of oxygen with hydrogen results in pressure loss as explained in Section 4.2.1. This combination of pressure increase and pressure loss towards the end of charging results in non-linear pressure variation as simulated in the inset of Fig. 6 agrees well with the pressure measured in the nickel hydrogen battery. The loss of charge to oxygen evolution side reaction at the nickel hydroxide electrode and oxidation of hydrogen results in lower SOC, 83.7%, instead 90% SOC as shown in Fig. 6. It is noted that the calculated SOC represents the amount of hydrogen gas formed or oxidized including self discharge and recombination from initial pressure. The pressure decrease during the rest period was simulated accurately accounting for the pressure losses due to recombination following Eq. (7) and self discharge rate calculated from a different cycle at 90% SOC. The simulated pressure agrees well with measured pressure during the rest period as shown in inset of Fig. 6. The battery SOC decreased during rest period by about 1% corresponding to recombination and self discharge. During discharge, the pressure losses due to the remaining amount of oxygen recombining with hydrogen (Eq. (7)) and the simultaneous hydrogen oxidation per the discharge process according to Faraday's law and ideal gas law were simulated. It is noted that pressure loss is non-linear at the beginning of discharge and is accurately simulated as shown in the inset of Fig. 6. The battery SOC decreases to 0% SOC at the end of cycle. This simulation shows that the pressure analysis can be used to predict pressure of the nickel hydrogen battery cycled to different states of charge with rest period. Conversely, the measured pressure inside the battery can be utilized to gauge the SOC of the battery as shown in this analysis.

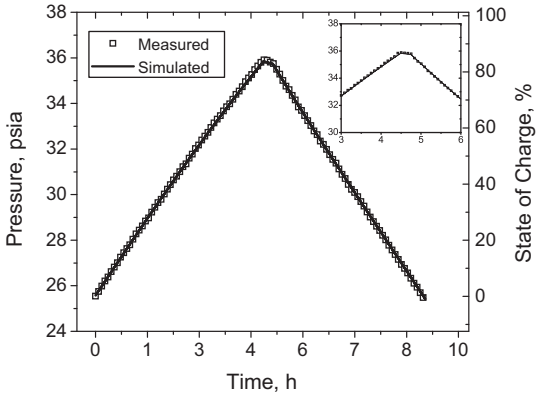

Fig. 6. Comparison of simulated pressure data to measured pressure data at C/5 rate to 90% SOC with 5 min rest period following charge.

4.4. Comparison of efficiency based on charge data and pressure data analysis

The coulometric efficiency for a charge–discharge cycle is calculated based on the charge passed and charge obtained during discharge as given by equation:

$$\eta_c = \frac{Q_{\text{discharge}}}{Q_{\text{charge}}} \tag{8}$$

In this case of the low pressure nickel hydrogen battery, coulometric efficiency can be expressed as follows:

$$\eta_c = \frac{Q_{\text{charge}} - Q_{O_2} - Q_{SD}}{Q_{\text{charge}}} \tag{9}$$

where Q_{O_2} is the charge lost to oxygen evolution and Q_{SD} is the charge lost to self discharge of the battery during the rest period. The amount of charge passed or charge lost due to oxygen evolution/self discharge can be expressed in terms of Faraday's law, $Q = \Delta nZF$. The amount of hydrogen formed during charging or oxygen evolved at the positive electrode or hydrogen oxidized due to self discharge is given ideal gas law: $\Delta n = \Delta PV/RT$. Applying above equations in Eq. (9) and with further simplification gives the following equation

$$\eta_c = \frac{\Delta P_{H_2} - 2\Delta P_{O_2} - \Delta P_{SD}}{\Delta P_{H_2}} \tag{10}$$

where ΔP_{H_2} is the pressure change corresponding to hydrogen formation during charging, ΔP_{O_2} is the pressure change due to oxygen evolution during charging and ΔP_{SD} is the pressure loss due to hydrogen oxidation in the rest period. The pressure change due to recombination calculated during the charge and rest period is the amount of hydrogen oxidized according to Eq. (5). The pressure change corresponding to oxygen evolution is equal to one half of the hydrogen oxidized due to recombination (ΔP_{Recom}) during charge and the rest period. The coulometric efficiency calculated based on the pressure loss is given by the following equation:

$$\eta_c = \frac{\Delta P_{H_2} - \Delta P_{\text{Recom}} - \Delta P_{SD}}{\Delta P_{H_2}} \tag{11}$$

The coulometric efficiency calculated based on 'charge passed and charge obtained during discharge' is compared to the coulometric efficiency obtained by pressure data analysis for a typical data set with 6 h rest period between charge and discharge in Fig. 7A. The estimated efficiency based on the pressure data matches the efficiency based on the charge and discharge data for all depths of charge, validating the pressure data analysis. Small differences of about 2% are observed for the 70 and 90% SOC. The

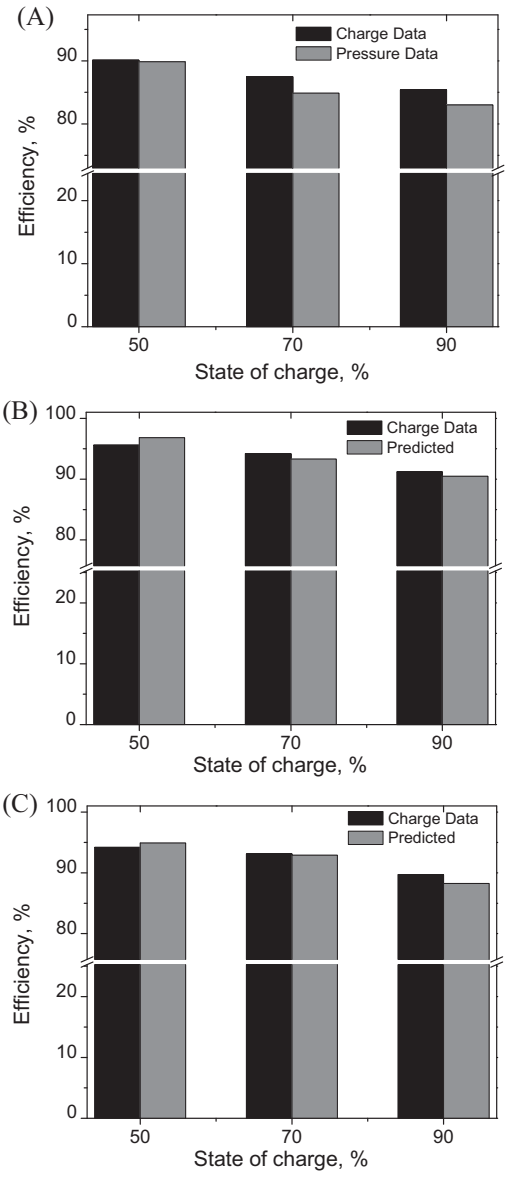

Fig. 7. Comparison of efficiency calculated based on the charge data and pressure data at different states of charge for different rest periods: (A) 6 h, (B) 5 min, and (C) 1 h. (A) Was calculated from pressure data measured for the charge discharge cycle with the 6 h rest period. (B) and (C) were predicted based on the 6 h rest period for 5 min and 1 h rest period cycles.

pressure data analysis slightly under predicts the actual coulometric efficiency observed. For a practical cell, under prediction would be preferred as opposed to over prediction of efficiency.

Next, the efficiency of the charge discharge cycles at different states of charge with 5 min and 1 h rest period were predicted without doing the in-depth pressure analysis for each cycle as described in the above sections. The only parameter used from the pressure data of the relevant cycle was the pressure drop due to recombination during charge. This was utilized to estimate the total pressure drop due to recombination (including rest period and discharge) based on the analysis of the cycle with 6 h rest period for different depths of charge (Table 2). The pressured drop corresponding to the amount of hydrogen oxidized during the 5 min and 1 h rest periods was determined from the self discharge rate calculated based on the 6 h rest period cycle at different depths of charge. The efficiency of the charge discharge cycle with 5 min and 1 h rest period was then predicted using Eq. (11) and is shown in Fig. 7B and C, respectively. The predicted coulometric efficiency without the in-depth pressure analysis agrees well with efficiency calculated based on the charge–discharge data.

Fig. 7 clearly shows that the efficiencies obtained from pressure data analysis are correct and supports the analysis of extracting the contributions of different mechanisms during charge and discharge of the nickel hydrogen cell. With the clear understanding of the pressure variations during charge, rest, and discharge, it is possible to use the pressure data, in addition to other methods, to reliably estimate the SOC of the nickel–hydrogen cells. In fact, the pressure data will be more reliable as it directly accounts for charge losses to self discharge and oxygen evolution occurring in the cell.

4.5. Ni–H_2 cell tests-below atmospheric pressure and without metal hydride

The performance of the nickel–hydrogen cell was also studied in the pressure range 0.4–1 atm. The cell was cycled to different states of charge with different rest periods between charge and discharge. The pressure data and the potential–current data were analyzed. The results obtained regarding the different mechanisms–self-discharge, oxygen evolution and recombination, were the same as presented above for cells tested at 2–3 atm.

5. Conclusions

A low pressure nickel hydrogen battery of 2–3 atm pressure was successfully assembled and tested. Coulometric efficiency calculated from potential–current data shows that the oxygen evolution increases with increasing SOC. The efficiency also decreases with an increase in the rest period after charge, indicating self-discharge of the nickel–hydrogen cell.

The pressure data measured simultaneously during charge, rest and discharge were analyzed. The results and analysis show that the oxygen evolution is observed at the end of charging and increases with SOC in agreement with the potential–current results. The evolved oxygen recombines with the hydrogen gas and about 70% of recombination occurs during the charge period. The rest of the recombination (30%) is complete in the first 1 h of the rest period after charging. The recombination time constant is large because the oxygen formed at the nickel hydroxide electrode has to diffuse to the platinum electrode. The self discharge rate was measured and is about C/117 at 90% SOC. The simulated pressure variation correlated with measured pressure and was utilized to estimate SOC of the battery.

The coulometric efficiency calculated from the pressure data analysis agrees well with coulometric efficiency calculated based on the potential–current data. The SOC of the Ni–H_2 cell can be accurately estimated by monitoring the cell pressure in addition to the existing methods like voltage measurements and coulomb counting.

Acknowledgment

This research was supported by NIH grant, NINDS R02-NS41809.

References

[1] K. Wang, C.-C. Liu, D.M. Durand, IEEE Trans. Biomed. Eng. 56 (2009) 6–14.
[2] P.H. Peckham, J.S. Knutson, Annu. Rev. Biomed. Eng. 7 (2005) 327–360.
[3] J.D. Dunlop, J.N. Brill, R. Erisman, in: D. Linden, T.B. Reddy (Eds.), Handbook of Batteries, McGraw-Hill, New York, 2002, pp. 32.31–32.32.
[4] J.D. Dunlop, G.M. Rao, T.Y. Yi, NASA Handbook for Nickel–Hydrogen Batteries, NASA, Scientific and Technical Information Branch, Washington, DC, 1993.
[5] J.J. Smithrick, P.M. Odonnell, J. Propul. Power 12 (1996) 873–878.
[6] L.H. Thaller, A.H. Zimmerman, Overview of the Design, Development, and Application of Nickel–Hydrogen Batteries, NASA, Glenn Research Center, Cleveland, OH, 2003.